Phys. Status Solidi A **206**, No. 6, 1273–1277 (2009) / **DOI** 10.1002/pssa.200881073

physica status solidi a
www.pss-a.com
applications and materials science

Terahertz transmission through p^+ porous silicon membranes

Shu-Zee A. Lo[*, 1], **Andrea M. Rossi**[1, 2], **and Thomas E. Murphy**[1]

[1] Department of Electrical and Computer Engineering, University of Maryland, College Park, MD 20742, USA
[2] Nanotechnology Department, Istituto Nazionale di Ricerca Metrologica, Torino, Italy

Received 24 March 2008, revised 31 October 2008, accepted 17 November 2008
Published online 5 February 2009

PACS 61.82.Rx, 78.55.Mb, 81.05.Rm, 81.16.–c, 87.50.U–

[*] Corresponding author: e-mail alenciou@umd.edu, Phone: +1 301-405-3602, Fax: +1 301-314-9281

We report an experimental measurement of far infrared dielectric properties of p^+-doped free-standing porous silicon membranes, characterized using terahertz time-domain spectroscopy. Freshly fabricated hydrogen-terminated porous silicon samples exhibited significant absorption in the terahertz regime, and the absorption was observed to slowly drift in response to the surrounding environment and the duration of illumination. Samples that are partially oxidized, either by age or through thermal oxidation in an oven, become almost transparent in the terahertz spectral regime, and the dielectric properties stabilize to a constant value. The partially-oxidized porous silicon samples are observed to have an absorption coefficient of approximately 2 cm^{-1} over the range of 0–2 THz, which corresponds to an effective resistivity of $35 \pm 9\ \Omega$ cm, approximately four orders of magnitude higher than that of the crystalline silicon from which they were formed. Spectral transmission measurements further confirm that p^+ porous silicon has no significant absorption peaks or other spectral variation in the 0–2 THz regime. These findings suggest that p^+ porous silicon could be a useful material for fabricating future THz devices.

1 Introduction The terahertz region of the electromagnetic spectrum, lying between microwave frequencies (100 GHz) and photonic frequencies (30 THz, $\lambda = 10$ μm), is an attracting attention for a diverse range of future applications including spectroscopic chemical identification, wireless communication, concealed weapon detection and non-destructive evaluation. Despite recent advances in sources and detectors, many of the core components such as bandpass filters, resonant cavities, and impedance-matching layers that are commonplace in optical and microwave systems have yet to be translated to the THz regime. Two reasons for this are the very different wavelength scale in the terahertz regime, and the scarcity of suitably transparent materials with the required dielectric properties.

Microwave devices are typically manufactured using casting and micromachining technologies, while photonic devices are typically constructed using thin-film deposition and lithographic techniques borrowed from the semiconductor industry. Neither approach is appropriate for fabricating THz components, which require dimensions that are too large for thin-film lithographic fabrication but too small for conventional machining. Furthermore many materials that are transparent at optical or microwave frequencies exhibit high absorption in the terahertz regime [1].

Future terahertz devices will require new materials that can be (1) engineered to have a wide range of dielectric permittivities (2) transparent across a broad range of THz frequencies, (3) cheaply fabricated in relatively thick layers and (4) easily incorporated into complex multilayer structures. Although nature does not naturally provide such materials, nanoporous silicon is an attractive and versatile material that could potentially satisfy all of these criteria.

While many have investigated the optical and DC dielectric properties of porous silicon [2–5], there have been few measurements of porous silicon in the terahertz (far infrared) regime. Those measurements that have been reported have exclusively examined porous silicon fabricated from lightly-doped silicon substrates [6, 7]. Heavily doped p^+ porous silicon offers several advantages over lightly-doped porous silicon, including the ability to more easily

fabricate complex, thick multilayer structures that incorporate a wide range of porosities [5, 8].

We report here the first experimental terahertz transmission measurement of nanoporous silicon fabricated from p^+ porous silicon. While freshly-fabricated p^+ porous silicon exhibits significant absorption, partially oxidized porous silicon is largely transparent in the range from 0–2 THz, making it a strong candidate for use in future terahertz devices.

2 Fabrication Free-standing porous layers were electrochemically etched from single-crystal, ⟨100⟩ oriented boron doped p^+ silicon wafers. The p^+ wafers had resistivities ranging from 1–5 mΩ cm, which corresponds to a dopant concentration in the range of 10^{20} cm^{-3}. Note that wafers with this level of doping would be entirely opaque in the terahertz regime, because of absorption by free carriers.

The electrochemical etching was performed using a two-chamber electrochemical cell in which both front and rear chambers were filled with an electrolyte comprised of hydrofluoric acid, water, and ethanol in a 1:1:2 ratio in volume. Although the porosity can be controlled by adjusting the current density, in order to facilitate comparison all of the samples reported here were etched using the same current density of 80 mA/cm^2. The etching was carried out in the dark, using a sequence current pulses of 2 minute duration each, with a 1 minute pause between pulses to allow equilibration of the solution at the bottoms of the pores. The total etching time was approximately 20 minutes, which resulted in a porous layer approximately 65 µm thick. Using gravimetric measurements, the porosity was calculated to be 67% under these etching conditions.

Following layer formation, a strong current pulse of 360 mA/cm^2 was applied for 7 seconds in order to separate the porous layer from the substrate, resulting in a free-standing porous membrane. The resulting free-standing porous membrane was thoroughly rinsed in ethanol and dried in air at room temperature.

3 Terahertz transmission measurements Figure 1 depicts the terahertz time-domain system used to characterize the porous silicon samples [9–11]. The terahertz signal was generated by illuminating an indium-arsenide semiconductor surface at oblique incidence with

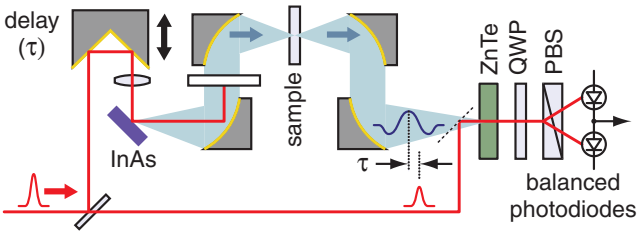

Figure 1 (online colour at: www.pss-a.com) Experimental setup used to measure terahertz transmission spectrum of porous silicon samples.

100 femtosecond optical pulses from a modelocked Ti:sapphire laser. The optical pulses are absorbed at the surface of the InAs, producing electrons and holes that diffuse at different rates into the semiconductor [12]. Because the generated electromagnetic pulse has sub-picosecond duration, it contains frequency components extending into the terahertz regime.

The terahertz signal was collimated and then focused at normal incidence to a size of approximately 1 mm onto the free-standing porous silicon membrane by a pair of off-axis gold-coated parabolic mirrors. A complementary pair of mirrors is then employed to collect the transmitted beam and direct it to the receiver.

The terahertz receiver uses a conventional electrooptic sampling technique, in which the terahertz pulse modulates the birefringence of a 1 mm thick, ⟨100⟩-oriented ZnTe crystal [13]. This modulation is sensed by measuring the shift in polarization of a probe beam that is derived from the same Ti:sapphire laser used to generate the terahertz pulse. By scanning the delay τ between the pump pulse and the probe pulse, it is possible to directly measure the terahertz electric field temporal waveform. By computing the Fourier transform of this temporal waveform, one obtains the spectrum of the terahertz signal. By comparing the measured spectra with and without the sample in place, one can compute the complete terahertz transmission spectrum of the sample.

4 Results and discussion Figure 2a shows the transmitted terahertz waveform measured before the porous silicon sample was introduced (upper trace) and after a freshly-fabricated, hydrogen-terminated porous silicon sample is inserted into the beam (lower trace). While the overall shape of the transmitted terahertz pulse remains approximately unchanged, the pulse amplitude decreases as a result of attenuation in the membrane and reflection at the surface. Also, the pulse position shifts to a later time because of the delay associated with propagation through a membrane with refractive index larger than that of air.

The amplitude of the transmitted terahertz pulse was observed to slowly drift over time. To illustrate this effect, Fig. 2b plots the peak amplitude of the transmitted terahertz signal, observed over a continuous two hour time interval. Point (A) indicates when the porous membrane was inserted into the terahertz beam, and point (B) marks the time when it was removed. All values plotted are normalized to the peak value of the terahertz field prior to insertion. During the 60 minute period while the sample is inserted, the transmitted amplitude falls monotonically from 0.30 to 0.19. The amplitude returns to its original level upon removal of the sample, indicating that the observed decrease cannot be attributed to systematic measurement drift.

The exact mechanism for this instability in absorption remains unclear, however we confirmed that the effect is localized in the region that is illuminated by the terahertz beam. That is, if the porous membrane is laterally dis-

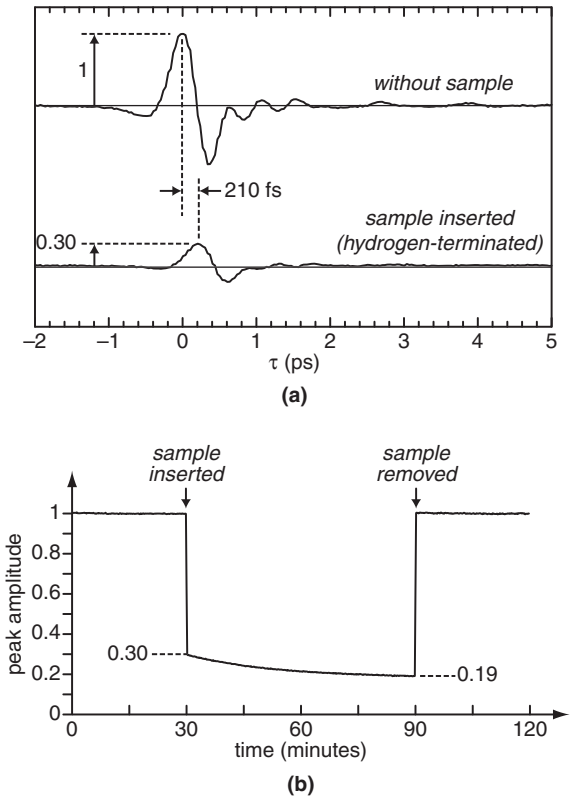

Figure 2 Terahertz transmission through freshly-fabricated, hydrogen-terminated porous silicon membrane. (a) Transmitted terahertz time-domain trace without (upper) and with (lower) the porous silicon inserted. (b) Peak amplitude of the transmitted THz pulse observed continuously during a 60 minute exposure time.

placed so that the terahertz beam samples a different area of the membrane, the transmitted amplitude returns to its original level and re-traces a similar downward evolution. While strong thermal effects have been reported for porous silicon in the past [14], the average power in our THz beam is at the μW level which we believe is unlikely to cause significant heating. The effect may be caused by a photo-induced (or THz-induced) change in the reactivity between the surface and the ambient environment.

This instability is also observed to diminish over time, as the highly-reactive hydrogen-terminated silicon surface slowly becomes replaced with more stable oxide termination. Figure 3 plots the normalized peak amplitude of the transmitted terahertz signal as a function of age for up to 13 days after initial fabrication. On each day of observation, the porous membrane was illuminated for a duration of 60 minutes and the peak amplitude of the transmitted terahertz pulse was recorded at the beginning (squares) and end (circles) of the 60 minute interval. While in each measurement, the transmitted amplitude decreases with exposure, on a longer timescale the sample slowly becomes more transparent and the initial and final amplitudes eventually converge to a relative transmission amplitude of

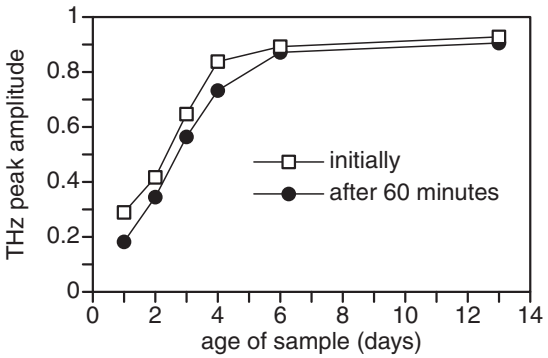

Figure 3 Normalized peak amplitude of the transmitted terahertz signal as a function of age for up to 13 days after initial fabrication. The squares indicate the initial amplitude and the circles show the amplitude after 1 hour of exposure.

0.90. This process can be accelerated by partially oxidizing the sample in a furnace, which yields stable, repeatable transparent porous silicon layers.

The refractive index and absorption coefficient (α) of the porous material can be estimated from the delay and attenuation of the terahertz pulse, respectively, as long as the thickness of the sample is known. However, a more accurate analysis should also account for the Fresnel reflection from the front and rear surfaces, and the multiple internal reflections that could occur inside of the membrane. Accounting for these effects, the complex amplitude transmission function is predicted to be [15, 16]

$$T(\omega) = \frac{4\tilde{n}}{(\tilde{n}+1)^2} \frac{\mathrm{e}^{-j(\tilde{n}-1)\omega d/c}}{1-(\tilde{n}-1/\tilde{n}+1)^2\,\mathrm{e}^{-j2\tilde{n}\omega d/c}}, \quad (1)$$

where ω is the angular frequency, $\tilde{n}$ is the refractive index (which can be complex and frequency-dependent) and d is the thickness of the sample.

Whereas many spectroscopic measurement systems can only determine the power transmission coefficient, $|T(\omega)|^2$, terahertz time domain spectroscopy permits $T(\omega)$ to be directly measured by computing the complex Fourier transform of the transmitted waveforms. Figure 4 plots the magnitude and phase of the complex transmission function $T(\omega)$ obtained in this way, for both the hydrogen-terminated sample and the oxidized sample.

The optical properties of the porous membrane can then be determined by fitting the measured data to Eq. (1), after choosing a suitable model for $\tilde{n}(\omega)$. We adopted the hypothesis that the porous membrane can be modeled as a conductive material characterized by a permittivity ε_R and an equivalent resistivity ρ. Under this assumption, the complex permittivity and refractive index are given by,

$$\varepsilon(\omega) = \tilde{n}^2(\omega) = \varepsilon_R - j\frac{1}{\rho\varepsilon_0\omega}. \quad (2)$$

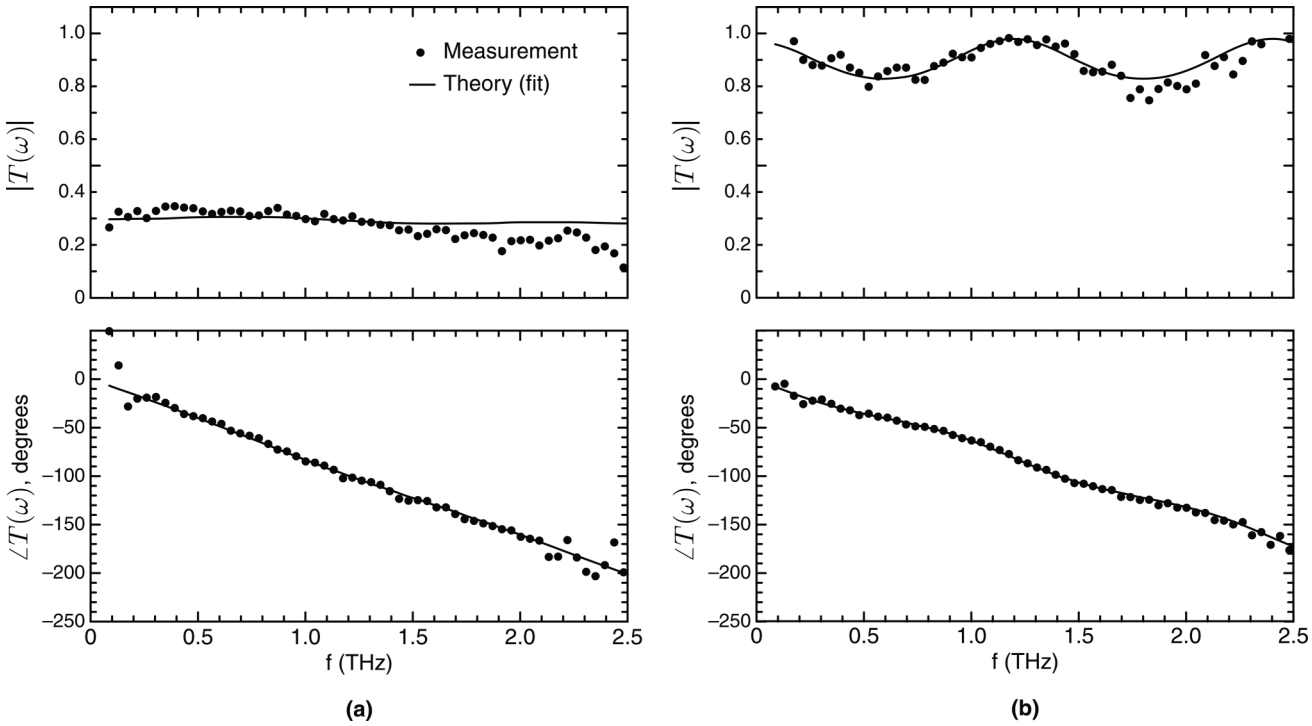

Figure 4 Magnitude (upper) and phase (lower) of the complex transmission function for (a) the freshly-made, hydrogen-terminated porous silicon membrane and (b) the partially oxidized porous silicon membrane. The solid points indicate the measured values, while the lines indicate the optimal linear least-squares fit to Eqs. (1) and (2).

We therefore seek to find the two unknown parameters ε_R and ρ that, when Eq. (2) is substituted into equation Eq. (1), yield the best fit to the measured data. These two parameters were determined by performing a weighted-nonlinear least-squares fit to the measured complex transmission function. The uncertainty in the fitting parameters was estimated by performing the same least-squares fit on five different data sets that were independently collected from the same sample. When performing the fit, the sample thickness d was treated as a known parameter which was measured separately.

For the freshly-fabricated, hydrogen-terminated porous silicon membrane, which had a measured thickness of 63 μm, we obtain $\varepsilon_R = 4.24 \pm 0.08$ mΩ cm and $\rho = 500 \pm 10$ mΩ cm. The solid lines in Fig. 4a show the function $T(\omega)$ calculated using these two parameters, which gives a reasonable fit to the experimental measurements. We note that the equivalent resistivity of the sample is more than two orders of magnitude higher than that of the bulk silicon from which the sample was formed. Nonetheless, the sample still exhibits significant loss across the THz spectral range.

For the oxidized porous silicon membrane, which had a thickness of 68 μm, we obtain $\varepsilon_R = 3.32 \pm 0.07$ Ω cm and $\rho = 35 \pm 9$ Ω cm. When substituted into Eqs. (1) and (2), these parameters give excellent agreement with the measured complex transmission spectrum, as shown in Fig. 4b. The sinusoidal shape of the transmission spectrum is explained by Fabry–Pérot fringes associated with multiple internal reflections inside of the 68 μm thick porous membrane. We note that the oxidized sample exhibits an equivalent resistivity that is more than four orders of magnitude larger than the original silicon substrate, yielding a low-loss dielectric material throughout the range from 0–2 THz.

The observation of a dramatic increase in resistivity in mesoporous silicon, compared to the crystalline silicon substrate has been well established in DC measurements [17–19], where resistivities in the range of 10^4–10^8 are routinely reported. Our results indicate a more modest, but still significant increase in resistivity at THz frequencies, although it must be pointed out that our results were inferred from transmission measurements in which all observed loss is ascribed to conductivity in the sample.

Figure 5 plots the predicted index of refraction (the real part of $\sqrt{\varepsilon}$) and the loss coefficient α as a function of frequency for the hydrogen-terminated porous silicon and the oxidized porous silicon. These curves were calculated from the complex permittivity (Eq. (2)), using the best-fit parameters. To better reflect the uncertainty, we calculated n and α by least-squares fitting to five independently-collected data sets. The gray region indicates the full range of values spanned by these five independent fits. The loss α for the oxidized case is especially difficult because the sample is too thin to yield measurable absorption.

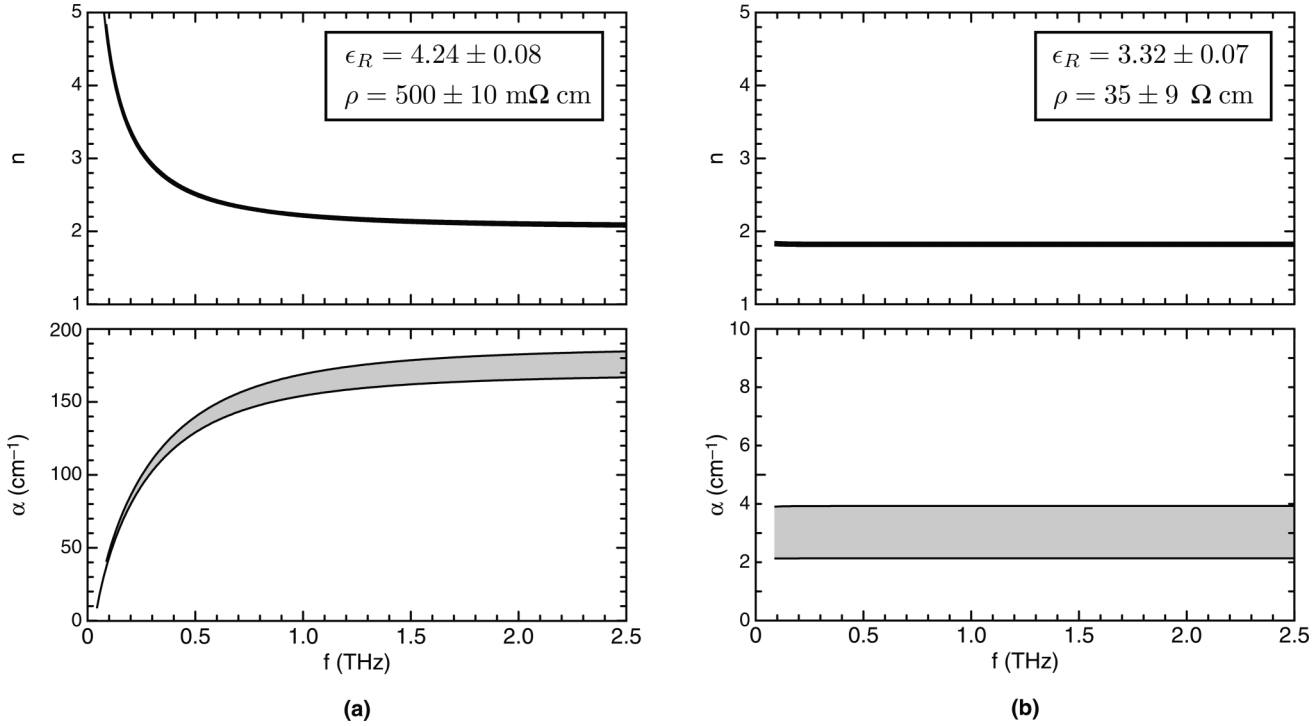

Figure 5 Predicted index of refraction (the real part of $\tilde{n}(\omega)$) and the loss coefficient α for (a) the freshly-fabricated hydrogen terminated porous silicon membrane and (b) the oxidized porous silicon membrane. The gray shaded region indicates the region of uncertainty.

5 Conclusions We describe the first experimental measurement of the dielectric properties of p^+ porous silicon in the terahertz (far infrared) spectral regime. In all cases, the free-standing porous silicon membranes exhibited less loss than the heavily-doped crystalline silicon from which they were fabricated. However, we observed distinctly different behavior between the freshly-fabricated, hydrogen-terminated porous membranes and oxidized porous samples. While freshly-fabricated samples have optical properties that are unstable and change with time, partially oxidized porous silicon samples exhibit excellent stability and almost negligible loss across a broad range of THz frequencies. This result suggests that oxidized porous silicon could serve as a useful and versatile material for fabricating multilayer terahertz devices.

References

[1] D. Grischkowsky, S. Keiding, M. van Exter, and C. Fattinger, J. Opt. Soc. Am. B **7**(10), 2007–2015 (1990).
[2] L. Pavesi, Riv. Nuovo Cimento **20**, 1–76 (1997).
[3] W. Theiß, Thin Solid Films **276**(1), 7–12 (1996).
[4] A. G. Cullis, L. T. Canham, and P. D. J. Calcott, J. Appl. Phys. **82**(3), 909–964 (1997).
[5] S. Frohnhoff and M. G. Berger, Adv. Mater. **6**(12), 963–965 (2004).
[6] L. Duvillaret, F. Garet, and J. L. Coutaz, IEEE J. Sel. Top. Quantum Electron. **2**(3), 739–746 (1996).
[7] S. Labbé-Lavigne, S. Barret, F. Garet, L. Duvillaret, and J. L. Coutaz, J. Appl. Phys. **83**(11), 6007–6010 (1998).
[8] M. G. Berger, C. Dicker, M. Thönissen, L. Vescan, H. Lüth, H. Münder, W. Theiß, M. Wernke, and P. Gross, J. Phys. D **27**(6), 1333–1336 (1994).
[9] B. Ferguson and X. C. Zhang, Nature Mater. **1**(1), 26–33 (2002).
[10] J. Shan, A. Nahata, and T. Heinz, J. Nonlinear Opt. Phys. Mater. **11**(1), 31–84 (2002).
[11] M. Hangyo, M. Tani, and T. Nagashima, Int. J. Infrared Millim. Waves **26**(12), 1661–1690 (2005).
[12] K. Liu, J. Xu, T. Yuan, and X. C. Zhang, Phys. Rev. B **73**, 155330 (2006).
[13] A. Nahata, A. S. Weiling, and T. F. Heinz, Appl. Phys. Lett. **69**(16), 2321–2323 (1996).
[14] H. Koyama and P. M. Fauchet, Appl. Phys. Lett **73**(22), 3259–3261 (1998).
[15] L. Duvillaret, F. Garet, and J. L. Coutaz, Appl. Opt. **38**(2), 409–415 (1999).
[16] K. Sakai (ed.), Terahertz Optoelectronics (Springer, 2005), chap. Terahertz time-domain spectroscopy, pp. 203–270.
[17] V. Lehmann, F. Hofmann, F. Möller, and U. Grüning, Thin Solid Films **255**, 20–22 (1995).
[18] V. Y. Timoshenko, T. Dittrich, V. Lysenko, M. G. Lisachenko, and F. Koch, Phys. Rev. B **64**, 085314 (2001).
[19] L. A. Balagurov, D. G. Yarkin, and E. Petrova, Mater. Sci. Eng. B **69**, 127–131 (2000).